RESEARCH PAPER   OPEN ACCESS

Synthesis and characterization of sugarcane bagasse ash with chitosan composite by batch adsorption studies

S. Vainath Praveen[1], R. Krishnaveni[2], G. Annadurai[*1]

[1]*Sri Paramakalyani Centre of Excellence in Environmental Sciences, Manonmaniam Sundaranar University, Alwarkurichi, Tamil Nadu, India*

[2]*Department of Commerce, Balagan Saraswathi Arts and Science College for Women, Manonmaniam Sundaranar University, Mukkudal, Tamil Nadu, India*

Abstract

Textile effluents, containing high concentrations of synthetic dyes, pose significant environmental hazards due to their toxic, carcinogenic, and mutagenic properties. These dyes contribute to serious water pollution because of their intricate aromatic structures, which make them resistant to traditional water treatment techniques. This study focuses on creating a novel adsorption method for removing synthetic colors like Methylene Blue (MB) from aqueous solutions by doping chitosan with sugarcane bagasse ash. Sugarcane bagasse ash is added to chitosan, a naturally occurring poly-amino saccharide, to increase its adsorption potential. FTIR, TGA, SEM, TEM, and BET analysis are used to examine the structural, thermal, and morphological properties of the composite. The findings suggest that the sugarcane bagasse ash with chitosan composite is a feasible and economical way to treat dye- aqueous solutions since it has a significant bandgap value and superior catalytic characteristics when compared to chitosan alone. This strategy offers a sustainable way to use agricultural waste in addition to addressing water contamination.

*****Corresponding Author:** G. Annadurai ✉ gannadurai@msuniv.ac.in

Introduction

Wastewaters from the textile industry are ranked among the most harmful pollutants to the environment because of the high discharge volume of artificial colorants that are toxic and reactive. But there is also a steady rise in the industrial use of colors, which contributes to increased water pollution (Wang *et al.,* 2021). In actuality, even a very tiny amount of pigment in water can cause aesthetic issues because it is so noticeable. Humans who come into constant contact with organic chemicals, such colors, suffer negative consequences. An estimated 15% of all dyes produced worldwide are thought to be wasted throughout the printing and dyeing processes and end up in waterways. The majority of industrial wastewater frequently contains methylene blue (MB), the most prevalent color in effluents from the paper, printing, and textile industries (Sachin *et al.,* 2010, 2011). The presence of aromatic rings in the structures that make up the chromophore and polar groups in this effluent makes it challenging to completely remove Methylene Blue. As a result, chitosan-based adsorption of hazardous dyes garnered a lot of interest (Cai *et al.,* 2020). Adsorption, coagulation, electrochemical separation, and membrane separation are just a few of the physical or chemical methods currently in use. Each has pros and cons in terms of how well the water treatment system works for particular kinds of wastewater or coloring compounds. When chemicals are used for coagulation, a significant amount of sludge-containing chemicals are produced, which calls for appropriate waste disposal management and also Large effluent volumes containing different dyes can be quickly treated with membrane filtration; the only drawback is the high initial expenditures. Therefore, a new method must be developed to eliminate the pollution, even at ppm levels (Gao *et al.,* 2022). The effectiveness of adsorption processes depends critically on the absorbent material selected. Activated charcoal, zeolites, silica gel, and alumina were often utilized absorbent materials in wastewater treatment (Arunraj *et al.,* 2019). But because most of these absorbent materials are unaffordable, research has been spurred to develop an environmentally beneficial, economically viable, and industrially eco-friendly absorbent material for wastewater treatment. If the absorbent materials are waste and don't require any more costly processing.

Because of its nature, agricultural waste is favored as an economical absorbent material; additionally, the cost issue is mitigated by the fact that it requires less processing than industrial absorbent materials. Accordingly, there is a great chance that industrial and agricultural waste will be used as absorbent materials (Hoslett *et al.,* 2020).

Chitosan, a synthetic by-product of chitin deacetylation, is one of the naturally occurring poly-amino saccharides. An efficient and eco-friendly absorbent substance for eliminating dyes from water is chitosan. There are several applications for chitosan, including films, powder, and beads. Chitosan's adsorption ability can be increased and the sedimentation time shortened by combining it with other substances, such as organic composites (Wang *et al.,* 2023). Therefore, it would be considerably more effective to treat textile and industrial waste water by combining agricultural waste with chitosan. Additionally, it helps lessen the problem of industrial waste disposal, which contaminates the air, water, and land. In order to circumvent the problem of regeneration, industrial wastes have been suggested as absorbent materials for single-use items. According to Murali and Uma (2009), the filled absorbent material could be promptly disposed of by incorporation or landfill. Following treatment, the primed absorbent material can be properly disposed of by incineration or landfill (Fatma Mohamed *et al.,* 2022). In order to enhance the adsorption of methylene dye in wastewater, this study sought to alter the sugarcane bagasse biomass using chitosan (Roy *et al.,* 2022). As a result, several instrumental approaches are used to examine the structural, thermal, and morphological properties of the sugarcane bagasse ashes with Chitosan Composite. An attempt is being made to use a Chitosan Composite system to adsorb Methylene Blue from Sugarcane Bagasse Ash. There is additional

discussion of how the rate of Methylene blue adsorption is affected by a number of variables, including pH levels, absorbent dosages, Methylene blue concentrations, and time periods.

Materials and methods

Materials

The chemical used in this study includes chitosan, HCl, acetic acid and ethanol were procured from Himedia Private Ltd, Mumbai. These chemicals are analytical grade chemicals and were used in this experiment directly without any further purification.

Preparation of sugarcane bagasse ash

The Sugarcane waste material after the extraction of juice from the juice was collected from the local juice market of Alwarkurichi. In a typical preparation procedure, sugarcane bagasse was soaked for a period of 24 h in double deionized water to remove any dust particles. The sugarcane material was then dried and the fiber so obtained was taken. The sugarcane dry fiber was washed using water and then HCl. Then the fiber was dried in the hot oven at 150 °C for 2 and a half hour. The drying process was repeated. The soaked, dried sugarcane was then burnt in open air to obtain a black sugarcane bagasse ash.

Synthesis of sugarcane bagasse ash with chitosan composites

5g of chitosan was dissolved in 5% acetic acid and stirred for 30 minutes to dissolve the chitosan and 5g of sugarcane bagasse ash was added to the solution. The reaction was kept for about 2- 4 hours with constant stirring. The mixture was before calcinated at 200°C. The sugarcane bagasse ash with chitosan composite was synthesized.

Batch adsorption studies

The adsorption performance of synthesized sample was assessed by measuring the adsorption of methylene blue batch studies. In a typical process with sugarcane bagasse ash with chitosan composite was added to 100 mL of aqueous dye solution with different parameters like dosages (0.02, 04, 06, 08, 0.10 g/L) at pH 6.8, Temperature 30°C; pH (2, 4, 6,

8,10) at Temperature 30°C, 0.10g/L adsorbent dosage, pH 6.8; dye concentration (10, 20, 30, 40, 50 mg/L) at pH 6.8, Temperature 30°C, 0.10g/L adsorbent dosage; Time (0, 50, 100, 150, 200, 250 mints) at pH 6.8, Temperature 30°C, 0.10g/L adsorbent dosage. The suspension of absorbent and dye solution was agitated in the dark for 24 hrs to reach adsorption/desorption equilibrium. The concentration of dye solution in the supernatant was then measured using a UV-vis spectrophotometer, which has a distinctive absorbance at λmax = 665 nm. The adsorption efficiency was calculated using the formula mentioned below:

Adsorption efficiency: $C_o - C / C_o \times 100$ %

Where, C_o = initial dye concentration, and C = dye concentration of the adsorption

*Characterization of sugarcane bagasse ash with chitosan composite*

FTIR spectra at various wavelengths ranging from 4000 cm^{-1} to 500 cm^{-1} were used to characterize the appearance of functional groups on the surface of the chitosan, which was identified by modification of the dried and processed sugarcane bagasse ash with chitosan composite. The weight loss profile at different temperatures was displayed by the TGA thermogram of sugarcane bagasse ash with chitosan composite at a flow rate of 52.4 mL/min and at a heating rate of 46.8°/min in a nitrogen atmosphere. The physical characteristics of the chitosan composite, such as heat absorption, phase transition, and crystallization, were characterized using a differential thermal analyzer. In this study, the surface morphology and particle size distribution of the chitosan composite were characterized using a scanning electron microscope. High-resolution pictures taken with a JEOL3010 Transmission Electron Microscope (TEM) were used to assess the biocomposite's dimensions and form. Using adsorption-desorption of nitrogen at 77.350K, the surface area of sugarcane bagasse ash with chitosan composite was characterized using the Brunauer–Emmett–Teller (BET) analytical approach.

Results and discussion

Fourier transform infrared spectroscopy (FTIR)

Materials were characterized using Fourier Transform Infrared spectroscopy. As illustrated in Fig. 1, the FTIR spectra of sugarcane bagasse ash with chitosan composite, which was obtained within the 4000-450 cm^{-1} spectral range, showed the distinctive peaks of the corresponding adsorbent. For example, the chitosan composite showed prominent peaks at 3355.79 cm^{-1} and 3348.94 cm^{-1}, respectively, due to the hydroxyl group, O-H bond, which is likely attributed to adsorbed water. In contrast to similar earlier studies (Cardenas *et al.,* 2004; Moghaddam *et al.,* 2017), it is evident that the functional OH group absorption occurs in the area of (2000-1000) cm-1 stretching vibration in phenolic and aliphatic structures. The C-H interaction with the absorbent surface, which indicates the carbon dioxide of normal air, was responsible for the peak at the area of 2862.36 cm^{-1} for sugarcane ash containing chitosan. N−H bended 1° amine groups are represented by the peak in chitosan at 1580.79 cm-1, which shifted to 1601.35 cm-1 in the chitosan-incorporated sugarcane materials (Wong *et al.,* 2009). The presence of carbon molecules is confirmed by the distinctive band at 1423.17 cm^{-1} and 1375.19 cm^{-1}, which corresponds to the C−O bond. In chitosan, the bands at 1032.53 cm^{-1} were attributed to the C-O-C vibrational stretching of polysaccharides. In chitosan-incorporated sugarcane bagasse ash, these bands changed to 1025.68 cm^{-1} (Prabu and Nagarajan, 2012). At a wavenumber of 888.61 cm^{-1}, a new peak was produced for biochar containing chitosan, confirming the presence of glucosidic (β) connections between sugar units. Strong chitosan encapsulation on the sugarcane bagasse ash surface is indicated by several functional groups or peak positions that were altered in the chitosan-incorporated sugarcane. Since this bond prevents other factors from influencing the FTIR peak assignments for the chitosan surface, their intensities were used as a reference for comparing the relative intensities of other bands (Prabu and

Natarajan, 2012; Carrillo *et al.,* 2004). The FTIR peak assignments are based on the literature reported for related compounds (Sun *et al.,* 2004; Ciolacu *et al.,* 2011).
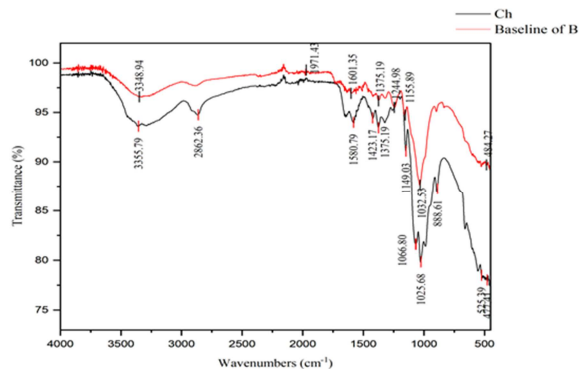

Fig. 1. Fourier transform infrared spectroscopy spectrum of sugarcane bagasse ash with chitosan composite

Thermogravimetric analysis (TGA)

Thermo Gravimetric Analysis was used to find the thermal strength of the particles at the different temperature ranges between 30°C to 700°C, with heating at a rate of 52.4 and 46.8°C min^{-1} beneath the flow of nitrogen inserted in Fig .2. A sharp weight loss of 73.46 mg was observed in the temperature range of 423 °C. Chitosan decomposes to produce CO_2, resulting in a weight loss of 50%. At 87.61 and 97.9°C, the initial reduction of weight was done by the dehydration of water particles in the material. The molecules broke down at 308°C and 341°C, which resulted in the following weight loss. Weakening of the bio composite is the cause of the final weight decrease. With weight loss on the TGA curve shown in Fig. 2, the desorption of water CO was physically adsorbed on the oxide surface, as indicated by the DTA curve, which revealed a single exothermic peak under 418°C and 573.5°C. This varying maximal breakdown was influenced by the residue (Zahra *et al.,* 2022). According to this study, sugarcane bagasse ash was effectively incorporated into the chitosan. A further characteristic of the DTA curves for sugarcane bagasse ash with chitosan composite is the loss of definition of the peaks at approximately 100°C and 800°C, which is evident in the case of synthesized particles. These peaks in the chitosan were linked to

interlamellar water loss and dehydroxylation from different settings (Corazzari *et al.,* 2013).
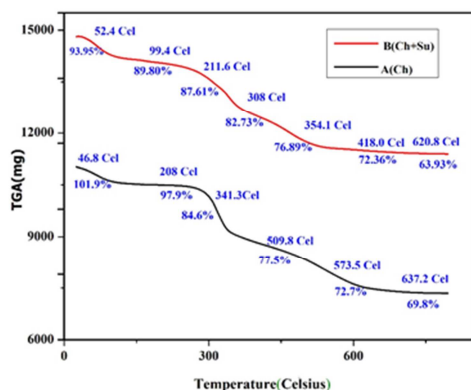
Fig. 2. Thermal gravimetric analysis of sugarcane bagasse ash with chitosan composite

According to the DTA curve for the samples in Fig. 3, the temperature stays constant during an endothermic transition that takes place at 300 °C. This temperature range is caused by water evaporating from the interspace and physiosorbed water that was adsorbed on the outside of the chitosan (Hong *et al.*, 2007; Corazzari *et al.*, 2015). For the produced composite, the second phase entails a multi-step dehydroxylation process at 400–500 °C.
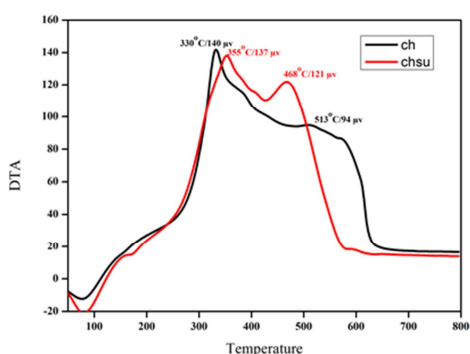

Fig. 3. DTA analysis sugarcane bagasse ash with chitosan composite

Scanning electron microscopy (SEM)
The morphological image of the synthesized particles, which are brilliant on the surface as seen in Fig. 4, is studied using scanning electron microscopy. The architecture of the synthesized particle was evident; it

had a smooth, flat surface with many porous pores, and its shape was mostly a membrane-like structure. Due to the adhesion of sugarcane baggage ash to the surface, the porous structure of chitosan was rough (Sharma and Bajpai, 2018). The bulk chitosan that is adhered to the surface does not alter the sugarcane baggage ash particles' porous structure. These results demonstrated the successful combination of chitosan with sugarcane baggage ash (Meryem Kerrou *et al.,* 2021).
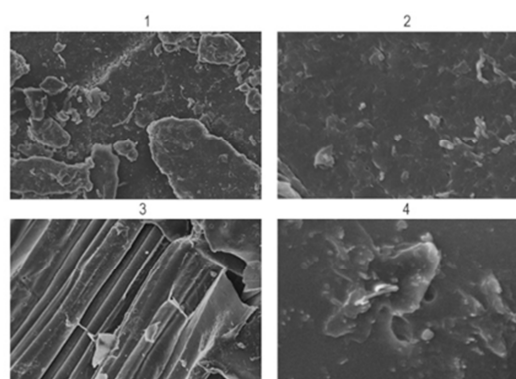

Fig. 4. SEM characterization chitosan (1) and sugarcane bagasse ash with chitosan composite (2)

The synthetic absorbents' surface morphology is rough and uneven, and because of their larger surface area, they have a significant potential for trapping and adsorbed dyes. As seen in Fig. 4, this morphology also indicates that the substance has a porous structure, indicating that the carbonaceous skeleton that makes up sugarcane baggage ash is what makes it up. Additionally, it was backed by the idea that a good absorbent should have a porous structure in order to boost surface area (Carvalho *et al.,* 2021). After being heated in a furnace while immersed in chitosan solution, the sugarcane baggage ash had significant pore development (Fig. 4), as well as an increased surface area and dye adsorption capability (Ximena Jaramillo-Fierro and Guisella Cuenca, 2024).

Energy dispersive x-ray analysis (EDAX)
Synthesized sugarcane bagasse ash doped with chitosan evidently contains both polymer and biochar in response to the EDX of the sugarcane bagasse ash with chitosan composite (Aftab *et al.,* 2022; Abdelwahaband nad Shukry, 2005; Hu *et al.,* 2007). As seen in Fig. 5, the

EDX spectrum is represented in multiple locations. Numerous mineral components were found in the chitosan-incorporated sugarcane bagasse ash according to elemental analysis, or EDX. High levels of C were found, followed by Mg, O, Cu, Si, Cl, and Ca.
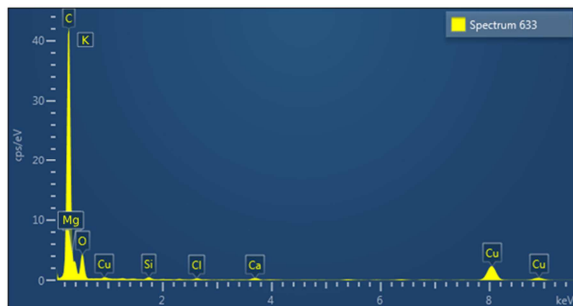
Fig. 5. EDAX pattern of sugarcane bagasse ash with chitosan composite
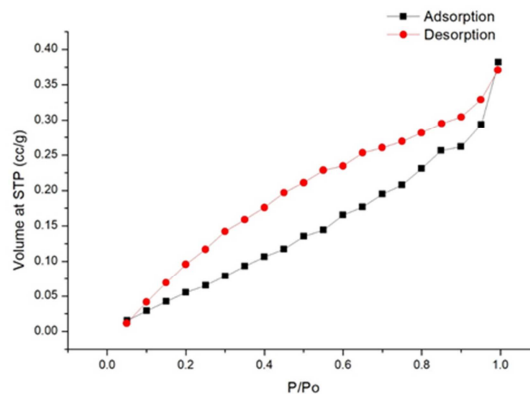
BET analysis of sugarcane bagasse ash with chitosan composite
Using a nitrogen adsorption-desorption isotherm recorded at 77.350K, the surface area, porosity size, and pore volume of sugarcane bagasse ash with chitosan composite were investigated (Fig. 6). The BET and BJH methods were used to measure the treated sample's surface area and pore size, respectively (Rhim *et al.,* 2006). The chitosan has an average surface area of 0.955 m²/g and a pore radius of 6.12 nm. As shown in Fig.6, the sugarcane bagasse ash with chitosan composite has a surface area of 19.047 m²/g and a pore radius of 0.299 nm.
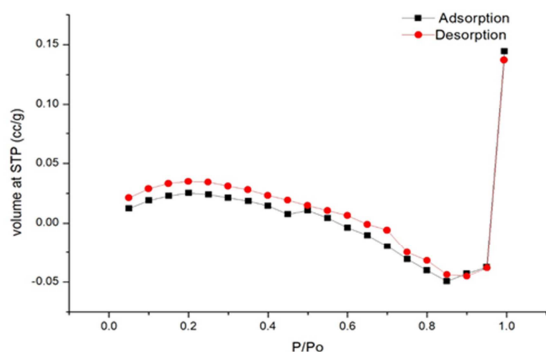
Fig. 6. BET analysis of sugarcane bagasse ash with chitosan composite characterized by nitrogen adsorption and desorption

According to the pore size distribution, the type I isotherm shows that chitosan has a microporous structure at its surface. According to the pore size distribution, the type IV isotherm shows that the chitosan-incorporated sugarcane bagasse ash has a mesoporous structure (Hung *et al.,* 2008). As illustrated in Fig. 7, the pore volumes of chitosan and sugarcane bagasse ash, as well as the chitosan composite that included sugarcane baggage ash, were 0.004 cc/g and 3.8058 cc/g, respectively. Chitosan-incorporated sugarcane bagasse ash was shown to have a larger surface area than chitosan alone. According to Arunraj *et al.* (2019), a material's greater surface area promotes the absorption of several chemicals and dyes.


Fig. 7. BET analysis of sugarcane bagasse ash with chitosan composite characterized by nitrogen adsorption and desorption

Similarly, chitosan-incorporated sugarcane bagasse ash with a larger surface area showed a lower pore radius. According to Ngamsurach *et al.* (2022), both of these characteristics affect how well chitosan-incorporated sugarcane removes dye or heavy metals, and it may be a better adsorbent for these removals than chitosan itself (Threepanich and Praipipat, 2021).

Effects of the sugarcane bagasse ash with chitosan composite dosage on the methylene blue adsorption
A pH of 7.0, an initial Methylene blue dye concentration of 10 mg/L, and a temperature of 30 °C were the experimental conditions used to examine the effects of

several dosages (0.04, 0.02, 0.06, 0.08, and 0.10 g/L) on the reaction rate (Fig. 8). Because there were more reaction sites and a higher absorbent concentration, the adsorption efficiency of Methylene blue rose dramatically with an increase in dosage (Sachin *et al.,* 2010). With a dosage of 0.10 g/L and a reaction period of 180 minutes, an adsorption efficiency of over 92.6% of Methylene Blue was obtained (Fig. 8). However, at a dosage of 0.06 g/L, the adsorption efficiency rose to 90%. Because there were more reactive sites available for electron transfer from the bio-composite's surface, the amount of methylene blue removed increased as the absorbent concentration rose (Mian and Liu, 2019). Because of their small size and large surface area, synthesized samples are highly effective at breaking down Methylene Blue. Based on these findings, 0.10 g/L of absorbent was found to be the ideal dosage for the ensuing Methylene Blue adsorption procedures.
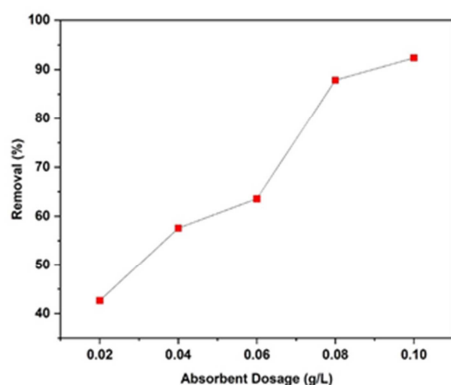

Fig. 8. Effects of the sugarcane bagasse ash with chitosan composite dosage on the adsorption of methylene blue

Effects of the pH levels on the methylene blue adsorption

According to numerous studies, the majority of advanced oxidation processes (AOPs) rely on pH levels that are conducive to the reaction. An essential factor that might influence the adsorption of organic pollutants in an acidic environment is pH, which can increase the number of reactive sites and, consequently, the amount of adsorption of these pollutants. The following experimental conditions were used to examine the impact of various pH levels

(2, 4, 6, 8, and 10) on the reaction rate (Liew Abdullah *et al.,* 2005): A dose of 0.10 g/L, a starting concentration of 10 mg/L of Methylene Blue, and a temperature of 30 °C. At an initial pH of 8, it was discovered that Methylene Blue's adsorption effectiveness was higher than 94% (Fig. 9). In a reaction, raising the pH from 8 to 10 decreased the adsorption effectiveness levels of methylene blue (Ho Thi Yeu Ly *et al.,* 2011). At pH 8, the maximum rate of methylene blue adsorption was attained. This could be because an alkaline pH causes metal oxides to be released on the absorbent surfaces, creating a large number of active sites for methylene blue dye reactions (Sivakami *et al.,* 2013; Wei and Qian, 2006).
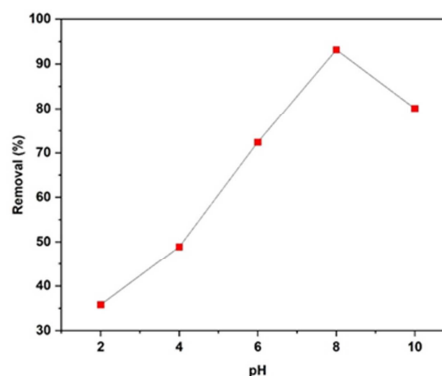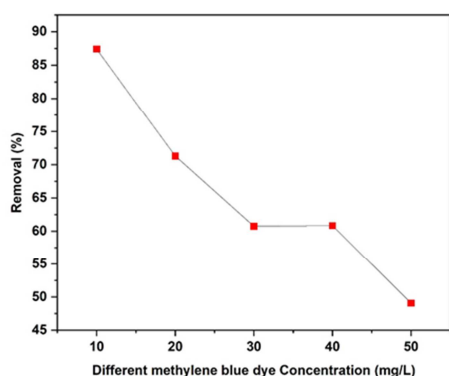

Fig. 9. Effects of the different pH on the adsorption of Methylene blue

At an initial pH of 8, it was discovered that Methylene Blue's adsorption effectiveness was higher than 94% (Fig. 9). In a reaction, raising the pH from 8 to 10 decreased the adsorption effectiveness levels of methylene blue (Ho Thi Yeu Ly *et al.,* 2011). At pH 8, the maximum rate of methylene blue adsorption was attained. This could be because an alkaline pH causes metal oxides to be released on the absorbent surfaces, creating a large number of active sites for methylene blue dye reactions (Sivakami *et al.,* 2013; Wei and Qian, 2006).

Effects of different blue adsorption dye concentrations

The following experimental conditions were used to examine the effects of different starting Methylene

blue concentrations (10, 20, 30, 40, and 50 mg/L) on the reaction rate: a pH of 7, a temperature of 30°C, and a dosage of 0.10 g/L. It was discovered that the residual amounts of Methylene Blue dye were 10, 20, 30, 40, and 50 mg/L, respectively (Fig.10). When the concentration was increased from 10 to 20 mg/L at a reaction, the adsorption efficiency of Methylene blue decreased from 87 to 70% (Saiful Azhar *et al.,* 2005).


Fig. 10. Effects of the different Methylene blue dye concentration on the adsorption

By raising the quantity of Methylene Blue dye, the number of active surface sites on the produced sample for the reaction was reduced. Methylene blue's adsorption onto the surfaces of the chitosan-based sugarcane bagasse ash is responsible for the decrease in the dye's adsorption rate. This is probably because it blocks the absorbent's active sites, which reduces the continuous production of hydroxyl radicals (Threepanich and Praipat, 2021).

Effects of different time on the Methylene blue adsorption
The following experimental conditions were used to examine the effects of time (0, 50, 100, 150, 200, and 250 minutes) on the reaction rate: a dose of 0.10 g/L, an initial pH of 7, a temperature of 30 °C, and an initial concentration of Methylene blue dye of 10 mg/L. The initial period, as shown in Fig. 11, had a very low rate of Methylene Blue adsorption, which may have been caused by a lack of hydroxyl radicals in the reaction (Chandraprabha *et al.,* 2012). The production of a significant amount of hydroxyl

radicals caused the methylene blue adsorption efficiency to increase from 20 to 83% with an increase in duration from 0 to 150 minutes. After 150 minutes, nevertheless, the efficiency remained consistent (Zahra *et al.,* 2022).
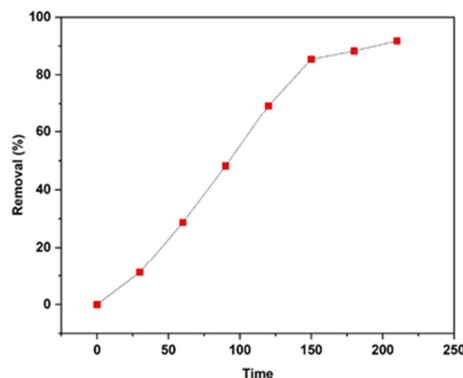
Fig. 11. Effects of the time on the adsorption of methylene blue

Conclusion
The functional groups were identified using FTIR spectra. EDAX analysis verified the presence of composition elements such Mg, O, Cu, Si, Cl, and Ca, and SEM images demonstrated that there is no agglomeration in the sugarcane bagasse ash with chitosan composite. The nitrogen adsorption-desorption isotherm on sugarcane bagasse ash with chitosan composite surface area was determined using the Bru-nauer–Emmett–Teller (BET) equation. The relative stability of the materials might be evaluated by thermogravimetric analysis. Utilizing agricultural waste, chitosan-based sugarcane bagasse ash was created. These particles demonstrated remarkable efficacy in aqueous Methylene Blue dye adsorption. Up until a certain point, increasing the absorbent's dosage increased the methylene blue adsorption rate; beyond that, it gradually declined. However, when the pH and initial concentration of Methylene Blue dye increased, so did the adsorption rate. A pH of 8.0, an initial Methylene blue dye concentration of 10 mg/L, sugarcane bagasse ash with chitosan composite doses of 0.10 g/L, and a temperature of 30°C were the ideal parameters for Methylene blue dye adsorption. The maximum

Methylene Blue adsorption rate was seen at an initial Methylene Blue dye concentration of 10 mg/L, which was followed by 93.6%. The hydroxyl radicals produced during the reaction are the most likely mechanism for the adsorption of Methylene Blue dye. According to the current study, methylene blue may be effectively eliminated from agricultural waste, making it a non-toxic, economical, and environmentally responsible method of treating wastewater. Lastly, the study's findings validate the scientific effectiveness of sugarcane bagasse ash and chitosan composite compounds as adsorbents in removing contaminants from water while also highlighting their sustainability and economic viability. By establishing the foundation for the future development of more affordable and sustainable water treatment technologies, this work opens up new avenues for addressing significant environmental challenges in the wastewater treatment sector.

References

Abdelwahab NA, Shukry N. 2015. Synthesis, characterization and antimicrobial properties of grafted sugarcane bagasse/silver nanocomposites. Carbohydrate polymers **115,** 276-284.

Aftab ZEH, Aslam W, Aftab A, Shah AN, Akhter A, Fakhar U, Khalid U. 2022. Incorporation of engineered nanoparticles of biochar and fly ash against bacterial leaf spot of pepper. Scientific Reports **12**(1), 8561.

Arunraj B, Sathvika T, Rajesh V, Rajesh N. 2019. Cellulose and *Saccharomyces cerevisiae* Embark to Recover Europium from Phosphor Powder. ACS Omega **4,** 940–952.

Cai X, Li J, Liu Y, Hu X, Tan X, Liu S, Luo L. 2020. Design and preparation of chitosan-crosslinked bismuth ferrite/biochar coupled magnetic material for methylene blue removal. International Journal of Environmental Research and Public Health **17**(1), 6.

Cardenas G, Miranda SP. 2004. FTIR and TGA studies of chitosan composite films. Journal of the Chilean Chemical Society **49**(4), 291-295.

Carrillo F, Colom X, Sunol J, Saurina J. 2004. Structural FTIR analysis and thermal characterization of lyocell and viscose-type fibres. European Polymer Journal **40**, 2229-2234

Carvalho JTT, Milani PA, Consonni JL, Labuto G, Carrilho ENM. 2021. Nanomodified sugarcane bagasse biosorbent: synthesis, characterization, and application for Cu (II) removal from aqueous medium. Environmental Science and Pollution Research **28**, 24744-24755.

Chandraprabha RD, Kanamadi TV, Ramachandra N, Ahalya, MN. 2012. Adsorption of methylene blue and amaranth on to tamarind pod shells. J Biochem Tech **3(**5), S189-S192.

Ciolacu D, Ciolacu F, Popa VI. 2011. Amorphous cellulose- structure and characterization. Cellulose Chemistry and Technology **45**(1-2), 13-21.

Corazzari I, Nisticò R, Turci F, Faga MG, Franzoso F, Tabasso S, Magnacca G. 2015. Advanced physico-chemical characterization of chitosan by means of TGA coupled on-line with FTIR and GCMS: Thermal degradation and water adsorption capacity. Polymer Degradation and Stability **112**, 1-9.

Fatma Mohamed, Mohamed Shaban, Shimaa Kotb Zaki, Maysaa SayedAbd-Elsamie, Radwa Sayed, Mohamed Zayed, Nermein Khalid, Sara Saad1, Sara Omar, Ashour M.Ahmed, AbanoubGerges, Abd El-Mageed, Soliman. 2022. Activated carbon derived from sugarcane and modifed with natural zeolite for efcient adsorption of methylene blue dye: experimentally and theoretically approaches. Scientifc Reports **12**, 18031.

Gao N, Du W, Zhang M, Ling G, Zhang P. 2022. Chitosan-modified biochar: Preparation, modifications, mechanisms and applications. International Journal of Biological Macromolecules **209**, 31-49.

Ho Thi Yeu Ly, Hoang Thi Khanh Dieu, Trinh Minh Tan Sang, Le Nguyen Minh Nha. 2011. Chemically modified sugarcane bagasse as a biosorbent for dye removal from aqueous solution. Chuyen San Khoa Hqc Tu NhienTap **2**(6), 175-181.

Hong PZ, Li SD, Ou CY, Li CP, Yang L, Zhang CH. 2007. Thermogravimetric analysis of chitosan. Journal of applied polymer science **105**(2), 547-551.

Hoslett J, Ghazal H, Mohamad N, Jouhara H. 2020. Removal of methylene blue from aqueous solutions by biochar prepared from the pyrolysis of mixed municipal discarded material. Science of the Total Environment **714**, 136832.

Hu Y, Du Y, Yang J, Kennedy JF, Wang X, Wang L. 2007. Synthesis, characterization and antibacterial activity of guanidinylated chitosan. Carbohydrate polymers **67**(1), 66-72.

Huang L, Zhai ML, Long DW, Peng J, Xu L, Wu GZ, Li JQ, Wei GS. 2008. UV-induced synthesis, characterization and formation mechanism of silver nanoparticles in alkalic carboxymethylated chitosan solution. Journal of Nanoparticle Research **10,** 1193-1202.

Liew Abdullah AG, Mohd Salleh MA, Siti Mazlina MK, Megat Mohd Noor MJ, Osman MR, Wagiran R, Sobri S. 2005. Azo dye removal by adsorption using waste biomass: Sugarcane Bagasse. International Journal of Engineering and Technology **2**(1), 8-13.

Meryem Kerrou, Najia Bouslamti, Abdelaziz Raada, Abdellah Elanssari, Driss Mrani, My Sliman Slimani. 2021. The Use of Sugarcane Bagasse to Remove the Organic Dyes from Wastewater. International Journal of Analytical Chemistry **5570806**, 1-11.

Mian MM, Liu G. 2019. Sewage sludge-derived $TiO_2/Fe/Fe_3C$-biochar composite as an efficient heterogeneous catalyst for degradation of methylene blue. Chemosphere **215**, 101-114.

Moghaddam L, Rencoret J, Maliger VR, Rackemann DW, Harrison MD, Gutiérrez A, del Río JC, Doherty WOS. 2017. Structural characteristics of bagasse furfural residue and its lignin component. An NMR, Py-GC/MS, and FTIR study. ACS Sustain Chem Eng **5**(6), 4846– 4855.

Murali K, Uma RN. 2009. Removal of Basic dye (Methylene Blue) Using Low Cost Biosorbent: Water Hyacinth. Int J Adv Engg Tech **4**, 386-391.

Ngamsurach P, Namwongsa N, Praipipat P. 2022. Synthesis of powdered and beaded chitosan materials modified with ZnO for removing lead (II) ions. Sci Rep **12**, 17184.

Prabu K, Natarajan. 2012. Isolation and FTIR spectroscopy characterization of chitin from local sources. Advances in Applied Science Research **3**(2), 1870-1875

Rhim JW, Hong SI, Park HM, Perry Ng KW. 2006. Preparation and characterization of chitosan-based nanocomposite films with antimicrobial activity. J Agric Food Chem **54**, 5814–5822

Roy H, Islam MS, Arifin MT, Firoz SH. 2022. Synthesis, characterization and sorption properties of biochar, chitosan and ZnO-based binary composites towards a cationic dye. Sustainability **14**(21), 14571.

Sachin M, Kanawade R, Gaikwad W, Misal S. 2010. Low cost Sugarcane Bagasse Ash as an Adsorbent for Dye Removal from Dye Effluent. International Journal of Chemical Engineering and Applications **1** (4), 309-318.

Sachin M, Kanawade R, Gaikwad W. 2011. Removal of Dyes from Dye Effluent by Using Sugarcane Bagasse Ash as an Adsorbent. International Journal of Chemical Engineering and Applications **2**(3), 202-206

Saiful Azhar S, Ghaniey Liew A, Suhardy D, Farizul Hafiz K, Irfan Hatim MD. 2005. Dye Removal from Aqueous Solution by using Adsorption on Treated Sugarcane Bagasse. American Journal of Applied Sciences **2**(11), 1499-1503.

Sharma M, Bajpai A. 2018. Superabsorbent nanocomposite from sugarcane bagasse, chitin and clay: Synthesis, characterization and swelling behaviour. Carbohydrate polymers **193**, 281-288.

Sivakami MS, Gomathi T, Venkatesan J, Jeong HS, Kim SK, Sudha PN. 2013. Preparation and characterization of nano chitosan for treatment wastewaters. International journal of biological macromolecules **57**, 204-212.

Sun JX, Sun XF, Zhao H, Sun RC. 2004. Isolation and characterization of cellulose from sugarcane bagasse. Polymer Degradation and Stability **84**, 331-339.

Threepanich A, Praipipat P. 2021. Powdered and beaded lemon peels-doped iron (III) oxide-hydroxide materials for lead removal applications: Synthesis, characterizations, and lead adsorption studies. J. Environ. Chem. Eng **9**, 106007.

Wang H, Xia H, Chen Q, Liu R, Zhang Y. 2023. Enhanced removal capacities and mechanisms of Mn/Fe-loaded biochar composites functionalized with chitosan Schiff-base or hydroxyl toward Pb (II) and Cd (II) from aqueous solutions. Journal of Environmental Chemical Engineering **11**(5), 111132.

Wang Z, Li Y, Xie X, Wang Z. 2021. Bifunctional MnFe2O4/chitosan modified biochar composite for enhanced methyl orange removal based on adsorption and photo-Fenton process. Colloids and Surfaces A: Physicochemical and Engineering Aspects **613**, 126104.

Wei D, Qian W. 2006. Chitosan-mediated synthesis of gold nanoparticles by UV photoactivation and their characterization. Journal of nanoscience and nanotechnology **6**(8), 2508-2514.

Wong SY, Tan YP, Abdullah AH, Ong ST. 2009. The Removal of Basic and Reactive Dyes Using Quartenised Sugar Cane Bagasse. Journal of Physical Science **20**(1), 59–74.

Ximena Jaramillo-Fierro, Guisella Cuenca. 2024. Enhancing Methylene Blue Removal through Adsorption and PhotocatalysisÍA Study on the GO/ZnTiO3/TiO2 Composite. Int. J. Mol. Sci **25**, 4367.

Zahra MH, Hamza MF, El-Habibi G, Abdel-Rahman AAH, Mira HI, Wei Y, Alotaibi SH, Amer HH, Goda AES, Hamad NA. 2022. Synthesis of a novel adsorbent based on chitosan magnetite nanoparticles for the high sorption of Cr (VI) ions: A study of photocatalysis and recovery on tannery effluents. Catalysts **12**(7), 678.